

## RESEARCH ARTICLE

# Molecular Docking studies reveals Rhein from rhubarb (*Rheum rhabarbarum*) as an effective inhibitor of ATP-binding Cassette Super Family G member 2

Muhammad Saad Khan<sup>#a</sup>, Bareera Mehmood<sup>#a</sup>, Qudsia Yousafi<sup>a</sup>, Shabana Bibi<sup>b</sup>, Sahar Fazal<sup>c</sup>, Shahzad Saleem<sup>a</sup>, Muhammad Wasim Sajid<sup>a</sup>, Awais Ihsan<sup>a</sup>, Muhammad Azhar<sup>\*a</sup>, Mohammad Amjad Kamal<sup>\*d,e,f</sup>

<sup>a</sup>Department of Biosciences, Faculty of Sciences, COMSATS University Islamabad, Sahiwal, Pakistan; <sup>b</sup>Department of Environment and life Engineering, Graduate School of Engineering, Maebashi institute of Technology, Maebashi, Japan; <sup>c</sup>Department of Biosciences, Faculty of Health and Life Sciences, Capital University of Sciences and Technology, Islamabad, Pakistan; <sup>d</sup>King Fahd Medical Research Center, King Abdulaziz University, P. O. Box 80216, Jeddah 21589, Saudi Arabia; <sup>e</sup>Enzymoics, 7 Peterlee Place, Hebersham, NSW 2770; <sup>f</sup>Novel Global Community Educational Foundation, Australia

**Abstract: Background:** ATP-binding cassette super family G2 protein is an active ATP-binding cassette transporter with potential to combat cancer stem cells.

**Objective:** Due to the lack of potential ATP-binding cassette super family G2 inhibitors we screened natural inhibitors, which could be safe source to control multidrug resistance by blocking the regulation of ATP-binding cassette super family G2 protein.

**Method:** Three-dimensional structure of ATP-binding cassette super family G2 protein downloaded from the protein databank and chemical structures of selected 166 compounds of the training dataset retrieved from PubChem. Drug-likeness and docking analysis shortlisted the dataset for pharmacophore generation. LigandScout 4.1.5 used for pharmacophore-based screening of Zbc library of ZINC database and Autodock Vina utilized for molecular docking against the predicted active pocket of the target protein to evaluate potential association of protein and ligands. Physicochemical properties of novel compounds calculated by admetSAR respectively.

**Results:** Through pharmacophore-based screening, ZINC4098704 (Rhein) was identified as a lead compound which demonstrates least binding energy (-8.5) and highest binding affinity with the target protein and showed optimal physicochemical profile. This compound is highly recommended for laboratory test to confirm its activity as ATP-binding cassette super family G2 inhibitors.

**Conclusion:** Our computer-based study systematically selected natural lead compound, which could be effective in inhibiting ATP-binding cassette super family G2 and may be helpful in reversing the effect of multidrug resistance in order to increase the effectiveness of chemotherapy in cancer treatment.

**Keywords:** ATP-binding cassette super family G-2 inhibitors, drug design, Cancer, Pharmacophore, Zbc-lead library.

---

**ARTICLE HISTORY**

---

Received:

Revised:

Accepted:

DOI:

# Equal First Author

\* Corresponding Author

## 1. INTRODUCTION

The Cancer is second most fatal cause of mortalities in under developed countries. In 2018, World health organization reported that the worldwide cancer patients expected to increase about 18.1 million, while the death rate of cancer patients increased to 9.6 million [1].

\*Department of Biosciences, Faculty of Sciences, COMSATS University Islamabad, Sahiwal, Pakistan; Phone/Fax: +92-40-4305005, Emails: [m.azhar@cuisahiwal.edu.pk](mailto:m.azhar@cuisahiwal.edu.pk).

\*King Fahd Medical Research Center, King Abdulaziz University, P. O. Box 80216, Jeddah 21589, Saudi Arabia; E-mails:

[prof.ma.kamal@gmail.com](mailto:prof.ma.kamal@gmail.com)

Due to recent advances in tumor research, information of different kind of tumors biological characteristics is improving constantly, such as tumors growth, cause of the abnormal cells development and dynamic alteration in the genomic structure of normal cells to abnormal [2].

Most common treatments of cancer are surgery, chemotherapy, different combination therapies and laser radiations. These treatments based on the improved outset of the biological and molecular genetics in tumor development [3]. Despite of all advancements the promising option for the cancer handling is still chemotherapy. But currently, 80-90% of deaths in the chemotherapy are due to drug resistance [4]. While huge number of abnormal cells become resistant to drugs becomes resistant during chemotherapy due to

certain drug administration. In this way drug resistance appears as a serious complication in dealing with cancer treatment [5]. Tumor heterogeneity could be the reason to cause resistance, under unrelated drug pressures. It could be more challenging when some of resistance pathways lead to multidrug resistance, increasing clinical complications which is difficult to overcome [6]. Cancerous drug resistance (DR) is a complex phenomenon. It could be subjective to different reasons like drug activation [7], drug target modification, increase or decrease of drug efflux, inhibition of cell expiry, repair of deoxyribonucleic acid (DNA), cell heterogeneity, and epigenetic properties or sometimes all these mechanisms could be the combined reasons of drug resistance in cancer patients and the main obstacle to effectively treat cancer [8]. It could be Multidrug resistance (MDR), described as resistance to physically and functionally distinct treatments to treat cancer cells. MDR is divided into two categories; intrinsic MDR and acquired MDR. Cancer microenvironment assortment indicates the expansion of intrinsic MDR, while acquired resistance is concerned to controlled chemotherapy. The main characteristics of MDR include abnormal growth of cancerous mass vasculature, aerobic glycolysis, areas of hypoxia with a small predisposition to cell death. To attain a lethal result for tumor mass, medications are

essential to lesser predisposition of abnormal cells and cell death [9].

Cellular and molecular process of MDR with respect to various drugs has comprehensively studied. Previous research demonstrated that experiments with drug-selected model cell lines proved increased expression of transporters superfamily known as ATP-binding cassette (ABC) with respect to breast cancer cell lines resistance macromolecular protein (ABCG2-ATP-binding cassette super family G2) [10], a most important reason to MDR. The increased expressions of ABCG2 on plasma membranes cause amplified efflux and reduction of intracellular accumulation of various discrete anti-cancer drugs, responsible of MDR [11].

For the management of various cancers, effective combinational therapy is required. Response to combinational therapy hindered by MDR in patients. Previous studies indicated that human ABCG2 protein is major reason of causing MDR due to which many combinations of chemotherapies failed to manage cancer. There is an urgent need to identify the potential inhibitors, which could inhibit the increased efflux of ABCG2. This study aims to screen natural library of drugs to identify potential lead compound based on the protein-ligand interactions, binding affinities and toxicity analysis by the implementation of

computer-aided drug design (CADD) pipeline.

## 2. MATERIALS AND METHOD

CADD scheme used in this study to screen ATP-binding cassette super family G 2 (ABCG2) inhibitors to manage multidrug resistance in treatment of cancer disease illustrated in Fig1.

### 2.1. Target protein selection

ABCG2 protein structure determined by electron microscopy was accessed from the freely available protein source; Protein data bank [PDB ID: 5NJ3] having 3.78Å resolutions [12] shown in Fig 2. Chimera [13] is used for visualization and determination of secondary structural features of target protein. Physiochemical properties of target protein were determined by ProtParam sequence analysis tool [14] (Table 1).

### 2.2. Training dataset selection for pharmacophore modeling

166 ABCG2 inhibitors against the ABCG2 target protein were identified by the literature review and their chemical structures were downloaded from PubChem database shown in Table 2 [15]. Two dimensional structures were downloaded and converted into three dimensional structures by using OpenBabel chemical toolbox [16] for further calculations. Drug-likeness and toxicity analysis was done by admetSAR [17] and those compounds which fulfil the drug-like properties and are not toxic were used for docking

analysis. A freely available tool Autodock Vina [18] was used for protein-ligand docking. Chemical structures and drug-like activities of selected top ten ABCG2 inhibitors along with summary of molecular docking results are shown in Table 3. These ten top scored ABCG2 inhibitors were selected for pharmacophore modeling [19].

### 2.3. Pharmacophore generation and screening of Zbc library of natural compounds

Ligand-based strategy is used to generate 3D pharmacophore model and virtual screening by LigandScout 4.1.5 [20]. This approach is used to search for common features against each ligand set. The training set consist of ten ABCG2 inhibitors (ligands) with maximum structural diversity and possessing inhibitory activity against ABCG2 target protein. Pharmacophore model was generated to analyze the shared features of selected ten ABCG2 inhibitors is shown in Fig 3 and used for the screening of Zbc library of natural compounds from ZINC database [21]. Pharmacophore features of the selected set of ABCG2 inhibitors with pharmacophore fit scores is shown in Table 4.

Table 5 demonstrates the overlay of selected set of ABCG2 inhibitors on the pharmacophore model created by LigandScout 4.1.5. Pharmacophore-based screening of 26432 compounds conducted by screening module of LigandScout 4.1.5. All identified virtual hits sorted according to their pharmacophore-fit score

and 10 virtual hits were selected for molecular docking simulations. Ten virtual hits were docked with the target protein and evaluated for binding energies and protein-ligand interactions by Autodock Vina [18] and LigPlot [22] respectively. Docking results of top 10 scored virtual hits screened from Zbc library shown in Table 6. Binding interactions of two potential virtual hits shown in Figure 4. An open source database admetSAR [17] is used to calculate the pharmacological properties [23] and toxicity profile of selected virtual hits. Table 7 shows pharmacological properties of top 10 scored virtual hits screened from Zbc library retrieved from ZINC database

### 2.4. Lead identification

Based on appropriate protein-ligand interactions and binding affinities with the special consideration of binding residues and in silico calculations of physicochemical parameters a lead compound was identified (Fig. 4), which could be a potential inhibitor of ABCG2 protein for the treatment of cancer.

## 3. RESULTS

Previous studies suggested that in cell survival of ABC transporters in the form of stress inducers might play additional roles that are not ABCG2 substrates (i.e., ionizing radiation, nutrient deprivation, and rapamycin). Various studies provide the evidence of ABCG2 inhibitors were more resistant to stressors in several cancer cell lines [24]. Our CADD scheme broadly used for potential virtual hits to lead

identification in pharmaceutical science is presented in figure 1. Most important methods of drug design; pharmacophore-based screening and structure-based analysis of protein-ligand complex are used to identify potential lead compound possessing the ability to inhibit the ABCG2 protein expression and could be useful in treatment of cancer.

### 3.1. Target protein selection

Three dimensional structure of target protein [PDB ID: 5NJ3] was retrieve from the protein data bank [12] and secondary structural features were determined and visualized by chimera tool [13] (Figure 2). The amino acid sequence of ABCG2 is 2198 residues long with 3.78 Å resolutions. The ABCG2 structure contains 32 helices, 10 sheets, beta-turn 85 and gamma turns 4 shown in the lower penal of Figure 2. Sequence analysis was conducted for calculation of physiochemical properties of ABCG2 protien using ProtParam [14] listed in Table 1. Because physiochemical properties of target protein understanding is advantageous for the drug development and in laboratory quality control procedure [25].

### 3.2. Training dataset selection

By the literature review, 166 ABCG2 inhibitors identified and their chemical information and two-dimensional structures retrieved against the ABCG2 target protein from PubChem. Dataset selected based on their inhibitory effect on ABCG2

involved in multi-drug resistance. Table 2 shows the ABCG2 inhibitors PubChem identifiers with their chemical names and their molecular weight.

Molecular properties of all compounds including molecular weight (MW), hydrogen bond donors (HBD) and hydrogen bond acceptors (HBA), log P, number of rings and rotatable bonds (RB), and polar surface area (PSA) predicted to fulfil the requirement of drug-likeness [26]. Among 166 compounds, 107 failed during Lipinski rule of five [27] and the most important is 59 drug-like compounds selected as a training set passed toxicity analysis. These 59 drug-like compounds subjected to interaction analysis with ABCG2 macromolecule.

### 3.3. Docking analysis of selected ABCG2 inhibitors dataset

Targeted docking was performed by using Autodock Vina [18] to find the potential interactions between ABCG2 macromolecule and ligand molecules. ABCG2 was used as a receptor protein. The selected 59 ABCG2 inhibitors were docked with ABCG2 protein and results of top-scored 10 compounds were showed with their binding energies ranging from -9.9 to -9.2 and binding interaction with in range of 4 Å. These ABCG2 inhibitors analyzed through LigPlot to determine the amino acids involved in protein-ligand binding interactions. Binding cavity of target protein shows Lys158, Glu191, Glu228, Ala230, Glu234, Lys276, Glu278 and Asp292 were the most common residues involved

in the binding interaction. The amino acids residues Glu228, Ala230, Glu234, Glu278 and Asp292 showed that the protein-ligand complex interactions were satisfying the binding pockets listed in Table 3.

### 3.4. Pharmacophore generation and screening of Zbc library of natural compounds

Based on least binding energies, top 10 selected ABCG2 inhibitors were subjected to generate best pharmacophore model. Ten pharmacophore models were generated their scores are presented in Figure 3 along with the proposed pharmacophore model presenting five common features; One yellow sphere having a blue small sphere in it representing hydrophobic region (HR) with an aromatic ring (AR), two red spheres represent the two HBA and one green sphere represents the HDB. Library of natural compounds (Zbc) of biogenic lead-like compounds, commercially available primary and secondary metabolites (natural products) were downloaded from ZINC database for virtual screening. After pharmacophore modelling, virtual screening performed via LigandScout 4.1.5 to identify the compounds that best align with respect to common features similar to those of pharmacophore model shown in figure 3. 18859 virtual hits (hit rate 71.35%) were identified out of 26432 compounds. Based on pharmacophore-fit score, top 10 compounds from Zbc library selected for molecular docking. Table 4 presents the pharmacophore features of the selected set of ABCG2 inhibitors with their

pharmacophore features and pharmacophore-fit scores for each selected set of ABCG2 inhibitors. Table 5 presents overlay of selected set of ABCG2 inhibitors upon two-dimensional and three-dimensional pharmacophore models with common features.

### 3.5. Docking analysis of screened virtual hits

Molecular docking of ABCG2 target protein with selected 10 virtual hits conducted using AutoDock Vina. Chemical structures of screened 10 virtual hits downloaded from ZINC database. These potential virtual hits with the least binding energies were identified as a result of docking simulations. Protein-ligand docked complexes were visualized by LigPlot and generates protein-ligands interactions diagrams to analyze the residues involve in binding interactions. ZINC44740 and ZINC4098704 virtual hits established least binding energies of -8.5. Asn604, Try91, Gln424, Thr607, Lys616 are important residues involved in interacting with binding pocket of ABCG2 protein (Table 6).

Molecular docking simulations identified the important residues interacting to create hydrophobic and hydrogen bonds with ABCG2 protein. Figure 4 demonstrates 2D and 3D presentation of two potential virtual hits docked with ABCG2 protein. In Figure 4 [A, C] ZINC44740 virtual hit shows two hydrogen bonds in the binding pocket of ABCG2 protein with Asn604 residue within distance of 2.80 Å and Try91 residue within

distance of 3.31 Å. While in Figure 4 [C, D] ZINC4098704 virtual hit shows four hydrogen bonds with Gln424 residue within distance of 2.93 Å, Thr607 residue within distance of 3.20 Å, Thr607 residue within distance of 2.95 Å and Lys616 residue within distance of 2.79 Å. Residues with the red projections involves in hydrophobic interactions.

### 3.6. Physicochemical calculations of selected virtual

Selected virtual hits were analyzed by passing through in silico drug-like filtration approach, Lipinski filter and toxicity analysis. These methods are very significant to screen large database of drug-like compounds to shortlist highly suitable virtual hits [28]. Physicochemical properties including Blood-Brain Barrier (BBB) [29], Human intestinal absorption (HIA) [30], Caco2 permeability, CYP450 2D6, AMES toxicity, and carcinogenicity were predicted to determine pharmacokinetics of the drug. Physicochemical properties and toxicity analysis of selected nine virtual hits is shown in Table 7.

### 3.7. Lead Identification

Among all the 161 chemical compounds from literature and PubChem database, some were according to the requirements of ADMET models and filtering rules as well as showing good binding energies, but they have some adverse side effects, which pose an obstacle in the inhibition of ABCG2. Therefore, selected lead compounds

ZINC4098704 (Rhein) [31] is a natural compound and consider to be safe source of medicine and it showed least binding energy and most favorable interactions may be considered as potential drugs against MDR caused by ABCG2.

## 4. DISCUSSION

Natural compounds and its derivatives most commonly used since long times are well known drugs for several killing disease [32]. In our previous studies we have demonstrated CADD pipelines to screen potential therapeutics for various killing diseases [33, 34]. Computer-based screening of large database of drug-like entities is most promising and compatible with different drug design and discovery methods to identify new drugs [35]. In the drug design procedures computer-based screening is mainly divided in to two types; molecular docking simulation and common feature pharmacophore based virtual screening [36].

To find potential natural ABCG2 inhibitors and to convey the knowledge of cancer drug design. We have used CADD methods in our study presented in Figure 1. Docking and pharmacophore approach has applied to the selected dataset of ABCG2 inhibitors to elucidate their behavior with respect to protein target ABCG2. Docking technique has been practiced to the selected dataset of 166 ABCG2 inhibitors and screened the 10 top score inhibitors with significant binding interactions and used for the ligand-based pharmacophore modeling to generate best

pharmacophore model which demonstrates the inhibition of the over expression of ABCG2 protein. One top score hypothetical common feature pharmacophore model is selected and used to screen the library of natural compounds to identify the potential virtual hits against ABCG2 target protein and selected 10 top scored virtual hits and subjected to molecular docking for the analysis of its structural insights with respect to ABCG2 protein. Physicochemical properties of the selected 10 virtual hits calculated to confirm its activity with respects to medicinal prospective. These selected 10 virtual hits could be developed in the wet lab and confirm its anti-cancer activity.

Structure-based calculation is appreciated if the molecular structure of protein is offered by protein databases [37]. In this CADD pipeline, a typical 3D protein structure PDB ID: 5NJ3 used for macromolecular interaction analysis [12]. Figure 2 shows that molecular target protein structure showing important structural features (32 helices, 10 sheets, beta-turn 85 and gamma turns 4) generated by chimera tool [13]. Physicochemical properties of target protein is an important factor to understand the behavior of protein with respect to drug development in laboratory for further procedures [25]. Physicochemical properties of target protein calculations demonstrated in Table 1. These properties consist of important chemical parameters such as molecular weight, number of protein atoms and total number of amino

acid residues and number of residues with respect to positive and negative charges, molecular formula of ABCG2 protein and theoretical isoelectric point, aliphatic index and instability index of ABCG2 protein.

By the literature review, 166 ABCG2 inhibitors based on their drug-likeness and their chemical information and two-dimensional structures retrieved against the ABCG2 target protein from PubChem. Selected dataset has shown inhibitory effect on ABCG2 protein involved in multi-drug resistance. Inhibitors identifiers with their chemical names and their molecular weight is shown in Table 2. Despite of all molecular and experimental information of cancerous drugs, still certain drugs could not fulfil the requirement of cancer treatment [38] and production of an effective drug is very expensive and time-consuming procedure and when subjected to the clinical trials fails due to its efficiency [39]. So physicochemical properties of all inhibitors calculated very carefully, out of 166 compounds 107 failed during Lipinski filtrations and toxicity predictions. 59 ABCG2 inhibitors fulfil the drug-like properties and subjected to molecular docking for interaction analysis with the ABCG2 protein. Mode of binding interactions in the cavity of ABCG2 protein was performed by Autodock Vina [18]. The selected ABCG2 inhibitors docked with ABCG2 and resulted with significant binding energies ranging -9.9 to -9.2. Docked complexes visualized by LigPlot to

determine the protein-ligand interactions. Lys158, Glu191, Glu228, Ala230, Glu234, Lys276, Glu278 and Asp292 residues were involved in interacting with the target protein. The amino acids residues Glu228, Ala230, Glu234, Glu278 and Asp292 are the important residues involved in inhibiting the expression of ABCG2 protein shown in Table 3. From the result of docking simulations 10 top score inhibitors were selected for pharmacophore modeling.

Development of pharmacophore model is a significant idea in drug design/discovery and various studies proved the success rate of pharmacophore modeling in the design/discovery of potential drugs [40]. Based on least binding energies and significant binding interactions with the target protein, a hypothetical pharmacophore model generated by 10 top-scored ABCG2 inhibitors. All inhibitors aligned together and generated ten pharmacophore models. Pharmacophore features of the selected set of ABCG2 inhibitors with their pharmacophore fit scores shown in table 4. Pharmacophore model with the best score was used for screening of ZINC library of natural compounds which shared five common features; one yellow sphere having a blue small sphere in it representing HR with an AR, two red spheres represent the two HBA and one green sphere represents the HBD shown in Figure 3. Overlay of selected set of ABCG2 inhibitors upon the pharmacophore model generated, tabulated in Table 5. After pharmacophore modelling,

virtual screening performed to identify the compounds that have common features to those of pharmacophore model generated by ABCG2 inhibitors dataset. 18859 virtual hits with hit rate of 71.35% were acknowledged with the similar features out of 26432 compounds. Based on pharmacophore-fit score, 10 virtual hits selected for molecular docking to evaluate its behavior with ABCG2 protein. Chemical structures of screened virtual hits retrieved via ZINC database. ZINC44740 and ZINC4098704 revealed with the least binding energies of -8.5. Asn604, Try91, Gln424, Thr607, Lys616 are important residues involved in interacting with binding pocket of ABCG2 protein (Table 6).

Evaluation of ADMET (Absorption, Distribution, Metabolism, Excretion and Toxicity) properties is very important in the selection of suitable lead compound. The selected 10 virtual hits pass through Lipinski rule of five and the predicted values of the ADMET calculations are suitable shown in table 7.

The merit of natural drugs has demonstrated in certain fatal diseases [33]. The selected lead compounds ZINC4098704 is a natural compound with anti-cancerous properties also known as Rhein. Rhein is an extensively used medicinal herb possessing anti-cancerous properties, it inhibit the proliferation and metastasis in human cells [31]. Hence, it has proved our CADD pipelines successfully identified a lead compound with remarkable properties to

inhibit the ABCG2 protein to control MDR in cancer cell lines.

## CONCLUSION

By using computational techniques, we have successfully identified a natural virtual lead compound ZINC4098704 also known as *Rhein* (*Rheum rhabarbarum*). Selected virtual lead compound demonstrates suitable binding interactions with the ABCG2 target protein and acceptable ADMET profile. It is highly recommended to test this compound in laboratory to confirm its activity as a potential ABCG2 inhibitor, which could control over expression of ABCG2 protein and helpful in dealing with multidrug resistance in order to increase the effectiveness of chemotherapy for cancer patients.

## LIST OF ABBREVIATIONS

All abbreviation has explained first used in the text.

## CONFLICT OF INTEREST

The authors confirm that there is no conflict of interest, financial or other.

## ACKNOWLEDGEMENTS

All authors equally contributed to conceptualize and write this scientific piece of work.

## REFERENCES

- [1] International Agency for Research on Cancer. Latest Global Cancer Data: Cancer Burden Rises to 18.1 Million New Cases and 9.6 Million Cancer Deaths in 2018. *Press Release*. 2018, pp 1–3.
- [2] MacConaill, L. E.; Garraway, L. A. Clinical Implications of the Cancer Genome. *J. Clin. Oncol.* **2010**, *28* (35), 5219.
- [3] Longley, D. B.; Johnston, P. G. Molecular Mechanisms of Drug Resistance. *J. Pathol. A J. Pathol. Soc. Gt. Britain Irel.* **2005**, *205* (2), 275–292.
- [4] Yuan, R.; Hou, Y.; Sun, W.; Yu, J.; Liu, X.; Niu, Y.; Lu, J.-J.; Chen, X. Natural Products to Prevent Drug Resistance in Cancer Chemotherapy: A Review. *Ann. N. Y. Acad. Sci.* **2017**, *1401* (1), 19–27.
- [5] Goodman, L. S.; Wintrobe, M. M.; Dameshek, W.; Goodman, M. J.; Gilman, A.; McLennan, M. T. Nitrogen Mustard Therapy: Use of Methyl-Bis (Beta-Chloroethyl) Amine Hydrochloride and Tris (Beta-Chloroethyl) Amine Hydrochloride for Hodgkin's Disease, Lymphosarcoma, Leukemia and Certain Allied and Miscellaneous Disorders. *J. Am. Med. Assoc.* **1946**, *132* (3), 126–132.
- [6] Zahreddine, H.; Borden, K. Mechanisms and Insights into Drug Resistance in Cancer. *Front. Pharmacol.* **2013**, *4*, 28.
- [7] Mansoori, B.; Mohammadi, A.; Davudian, S.; Shirjang, S.; Baradaran, B. The Different Mechanisms of Cancer Drug Resistance: A Brief Review. *Adv. Pharm. Bull.* **2017**, *7* (3), 339.
- [8] Housman, G.; Byler, S.; Heerboth, S.; Lapinska, K.; Longacre, M.; Snyder, N.; Sarkar, S. Drug Resistance in Cancer: An Overview. *Cancers (Basel)*. **2014**, *6* (3), 1769–1792.
- [9] Dinic, J.; Podolski-Renic, A.; Stankovic, T.; Bankovic, J.; Pesic, M. New Approaches with Natural Product Drugs for Overcoming Multidrug Resistance in Cancer. *Curr. Pharm. Des.* **2015**, *21* (38), 5589–5604.
- [10] Winter, E.; Gozzi, G. J.; Chiaradia-Delatorre, L. D.; Daflon-Yunes, N.; Terreux, R.; Gauthier, C.; Mascarello, A.; Leal, P. C.; Cadena, S. M.; Yunes, R. A.; et al. Quinoxaline-Substituted Chalcones as New Inhibitors of Breast Cancer Resistance Protein ABCG2: Polyspecificity at B-Ring Position. *Drug Des. Devel. Ther.* **2014**, *8*, 609–619.
- [11] Mo, W.; Zhang, J.-T. Human ABCG2: Structure, Function, and Its Role in Multidrug Resistance. *Int. J. Biochem. Mol. Biol.* **2012**, *3* (1), 1.
- [12] Taylor, N. M. I.; Manolaridis, I.; Jackson, S. M.; Kowal, J.; Stahlberg, H.; Locher, K. P. Structure of the Human Multidrug Transporter ABCG2. *Nature* **2017**, *546* (7659), 504.
- [13] Pettersen, E. F.; Goddard, T. D.; Huang, C. C.; Couch, G. S.; Greenblatt, D. M.; Meng, E. C.; Ferrin, T. E. UCSF Chimera—a Visualization System for Exploratory Research and Analysis. *J. Comput. Chem.* **2004**, *25* (13), 1605–1612.

- [14] Bairoch, A.; Gattiker, A.; Wilkins, M. R.; Gasteiger, E.; Duvaud, S.; Appel, R. D.; Hoogland, C. Protein Identification and Analysis Tools on the ExPASy Server. In *The Proteomics Protocols Handbook*; 2009; pp 571–607.
- [15] Kim, S.; Thiessen, P. A.; Bolton, E. E.; Chen, J.; Fu, G.; Gindulyte, A.; Han, L.; He, J.; He, S.; Shoemaker, B. A.; et al. PubChem Substance and Compound Databases. *Nucleic Acids Res.* **2015**, *44* (D1), D1202–D1213.
- [16] Banck, M.; Vandermeersch, T.; O’Boyle, N. M.; Hutchison, G. R.; Morley, C.; James, C. A. Open Babel: An Open Chemical Toolbox. *J. Cheminform.* **2011**, *3* (1), 33.
- [17] Cheng, F.; Li, W.; Zhou, Y.; Shen, J.; Wu, Z.; Liu, G.; Lee, P. W.; Tang, Y. AdmetSAR: A Comprehensive Source and Free Tool for Assessment of Chemical ADMET Properties. *J. Chem. Inf. Model.* **2012**, *52* (11), 3099–3105.
- [18] Trott, O.; Olson, A. J. Software News and Update AutoDock Vina: Improving the Speed and Accuracy of Docking with a New Scoring Function, Efficient Optimization, and Multithreading. *J. Comput. Chem.* **2010**, *31* (2), 455–461.
- [19] Milne, G.; Nicklaus, M.; in, S. W.-S. and Q.; 1998, undefined. Pharmacophores in Drug Design and Discovery. *Taylor Fr.*
- [20] Wolber, G.; Langer, T. LigandScout: 3-D Pharmacophores Derived from Protein-Bound Ligands and Their Use as Virtual Screening Filters. *J. Chem. Inf. Model.* **2005**, *45* (1), 160–169.
- [21] Irwin, J. J.; Shoichet, B. K. ZINC- A Free Database of Commercially Available Compounds for Virtual Screening. *J. Chem. Inf. Model.* **2005**, *45* (1), 177–182.
- [22] Wallace, A. C.; Laskowski, R. A.; Thornton, J. M. LIGPLOT: A Program to Generate Schematic Diagrams ... [Protein Eng. 1995] - PubMed Result. *Protein Eng.* **1995**, *8* (2), 127–134.
- [23] Daneman, R.; Prat, A. The Blood--Brain Barrier. *Cold Spring Harb. Perspect. Biol.* **2015**, *7* (1), a020412.
- [24] Mao, Q.; Unadkat, J. D. Role of the Breast Cancer Resistance Protein (BCRP/ABCG2) in Drug Transport— an Update. *AAPS J.* **2015**, *17* (1), 65–82.
- [25] Protein Physico-Chemical Properties. <http://www.intertek.com/pharmaceutical/biopharmaceuticals/protein-physicochemical/>
- [26] Mirza, M.; Ikram, N. Integrated Computational Approach for Virtual Hit Identification against Ebola Viral Proteins VP35 and VP40. *Int. J. Mol. Sci.* **2016**, *17* (11), 1748.
- [27] Lipinski, C. A.; Lombardo, F.; Dominy, B. W.; Feeney, P. J. Experimental and Computational Approaches to Estimate Solubility and Permeability in Drug Discovery and Development Settings. *Adv. Drug Deliv. Rev.* **1997**, *23* (1–3), 3–25.
- [28] Ntie-Kang, F.; Lifongo, L. L.; Mbah, J. A.; Owono, L. C. O.; Megnassan, E.; Mbaze, L. M.; Judson, P. N.; Sippl, W.; Efange, S. M. N. In Silico Drug Metabolism and Pharmacokinetic Profiles of Natural Products from Medicinal Plants in the Congo Basin. *silico Pharmacol.* **2013**, *1* (1), 12.
- [29] Ballabh, P.; Braun, A.; Nedergaard, M. The Blood–brain Barrier: An Overview: Structure, Regulation, and Clinical Implications. *Neurobiol. Dis.* **2004**, *16* (1), 1–13.
- [30] Wessel, M. D.; Jurs, P. C.; Tolan, J. W.; Muskal, S. M. Prediction of Human Intestinal Absorption of Drug Compounds from Molecular Structure. *J. Chem. Inf. Comput. Sci.* **1998**, *38* (4), 726–735.
- [31] Zhou, Y.-X.; Xia, W.; Yue, W.; Peng, C.; Rahman, K.; Zhang, H. Rhein: A Review of Pharmacological Activities. *Evidence-Based Complement. Altern. Med.* **2015**, 2015.
- [32] Lahlou, M. The Success of Natural Products in Drug Discovery. *Pharmacol Pharm* **2013**, *4* (3A), 17–

- 31.
- [33] Rizwan, S.; Mehmood, A.; Khalid, I.; Khan, M. S.; Yousafi, Q.; Kalsoom, S.; Rashid, H. Polypharmacology Approach Against Migraine with Aura and Brain Edema for the Development of an Efficient Inhibitor and Its Analogues. *Curr. Comput. Aided. Drug Des.* **2018**, *14* (4), 385–390.
- [34] Bibi, S.; Sakata, K. Current Status of Computer-Aided Drug Design for Type 2 Diabetes. *Curr. Comput. Aided. Drug Des.* **2016**, *12* (2), 167–177.
- [35] Bibi, S.; Sakata, K. An Integrated Computational Approach for Plant-Based Protein Tyrosine Phosphatase Non-Receptor Type 1 Inhibitors. *Curr. Comput. Aided. Drug Des.* **2017**, *13* (4), 319–335.
- [36] Chen, Z.; Li, H.; Zhang, Q.; Bao, X.; Yu, K.; Luo, X.; Zhu, W.; Jiang, H. Pharmacophore-Based Virtual Screening versus Docking-Based Virtual Screening: A Benchmark Comparison against Eight Targets. *Acta Pharmacol. Sin.* **2009**, *30* (12), 1694.
- [37] Fuller, J. C.; Burgoyne, N. J.; Jackson, R. M. Predicting Druggable Binding Sites at the Protein-Protein Interface. *Drug Discovery Today.* 2009, pp 155–161.
- [38] Hoelder, S.; Clarke, P. A.; Workman, P. Discovery of Small Molecule Cancer Drugs: Successes, Challenges and Opportunities. *Mol. Oncol.* **2012**, *6* (2), 155–176.
- [39] Fogel, D. B. Factors Associated with Clinical Trials That Fail and Opportunities for Improving the Likelihood of Success: A Review. *Contemp. Clin. trials Commun.* **2018**, *11*, 156–164.
- [40] Tuccinardi, T.; Poli, G.; Corchia, I.; Granchi, C.; Lapillo, M.; Macchia, M.; Minutolo, F.; Ortore, G.; Martinelli, A. A Virtual Screening Study for Lactate Dehydrogenase 5 Inhibitors by Using a Pharmacophore-Based Approach. *Mol. Inform.* **2016**, *35* (8–9), 434–439.



**Table 1. Physiochemical properties of ATP-binding cassette super family G 2 protein calculated by ProtParam**

Properties	Values
No. of amino acids	2198
No. of atoms	33907
Molecular Weight	241349.72
Theoretical PI	8.61
Negatively charged Residues	178
Positively Charged Residues	200
Aliphatic index	85.07
Instability index	34.30

Review Version

**Table 2. Selected ATP-binding cassette super family G2 inhibitors set with PubChem CID (Identifiers) with their chemical names and molecular weight.**

PubChem CID	Chemical Names	Molecular Weight	PubChem CID	Chemical Names	Molecular Weight
23676225	Equilin sodium sulfate	370.39	60956	Lurtotecan	518.57
3488	Glyburide	494.00	9955286	ME3277	448.45
11625818	Idelalisib	415.43	126941	Methotrexate	454.45
5351188	NSC73306	395.25	24466	Metoprime	269.13
9808844	Telatinib	409.83	4212	Mitoxantrone	444.49
6918316	Symadex	441.35	11667893	Motesanib	373.46
3054	(Z,E)-Diethylstilbestrol	268.36	9832912	Moxidectin	639.83
454858	1. (+)-FTC	247.24	5281078	Mycophenolate mofetil	433.50
17732	1. 4-HppH	268.27	439246	Naringenin	272.26
60863	5-amino orotate	500.51	9915861	NB-506	562.49
3385	5-Fluorouracil	130.08	64143	Nelfinavir	567.79
72271	7-Hydroxystaurosporine	482.54	4474	Nicardipine	479.53
72402	9-Aminocamptothecin	363.37	4485	Nifedipine	346.34
10184653	Afatinib	485.94	644241	Nilotinib	529.53
83969	Albendazole sulfoxide	281.33	4507	Nitrendipine	360.37
49806720	Alectinib	482.63	6604200	Nitrofurantoin	238.16
5287969	Alvocidib	401.84	4539	Norfloxacin	319.36
101524	Becatecarin	669.56	54675769	Novobiocin	612.63
60824	Befloxatone	349.31	4583	Ofloxacin	361.37
6456014	Belotecan	433.51	130881	Olmesartan medoxomil	558.59
68740	Zoledronic acid	272.09	4594	Omeprazole	345.42
9874592	Berubicin	633.65	71496458	Osimertinib	499.62
5351322	Bisantrene	398.47	40854	Oxfendazole	315.35
17989820	Boc-5-aminolevulinic acid	231.25	4679	Pantoprazole	383.37
644073	Buprenorphine	467.65	10113978	Pazopanib	437.52
6076	CAMP	329.20	16741	Phenethyl isothiocyanate	163.24
24360	Camptothecin	348.36	5323510	Pheophorbide a	592.70
156414	Canertinib	485.94	5480977	Phytoporphyrin	534.66
38904	Carboplatin	373.27	636397	Pirarubicin	627.64
446156	Cerivastatin	459.56	54369	Piritrexim	325.37
5479494	Chlorin e6	596.69	5282452	Pitavastatin	421.47
5997	Cholesterol	386.66	10205	Plumbagin	188.18
2756	Cimetidine	252.34	24826799	Ponatinib	532.57
2764	Ciprofloxacin	331.35	12594	Prasterone sulfate	368.49
20279	Cladribine	285.69	54687	Pravastatin	424.53
119182	Clofarabine	303.68	4893	Prazosin	383.41
16222096	Cobimetinib	531.32	4971	Protoporphyrin IX	562.67
969516	Curcumin	368.38	4993	Pyrimethamine	248.71
44462760	Dabrafenib	519.56	6918492	Pyropheophorbide a methyl ester	548.69
107971	Daidzin	416.38	5280343	Quercetin	302.24
56640146	Dasabuvir	493.58	5029	Rabeprazole	359.44
3062316	Dasatinib	488.01	104758	Raltitrexed	458.49

30323	Daunorubicin	527.53	11167602	Regorafenib	482.82
30323	Daunorubicin	527.53	65217	Rhodamine 123	380.83
3033	Diclofenac	296.15	493570	Riboflavin	376.37
219023	Diflomotecan	398.37	6451164	Rilpivirine	366.43
3108	Dipyridamole	504.64	5070	Riluzole	234.20
5484207	D-Luciferin	280.32	11304743	Riociguat	422.42
16078	Dronabinol	314.47	10311306	Rolapitant	500.48
443293	E3040 sulfate	379.45	446157	Rosuvastatin	481.54
9808998	Edotecarin	608.56	131682	Safinamide	302.35
119373	Elacridar	563.65	104842	SN 38 lactone	392.41
71188	Enrofloxacin	359.40	443154	SN-38 Glucuronide	568.53
41867	Epirubicin	543.52	45375808	SOFOSBUVIR	529.46
176870	Erlotinib	393.44	216239	Sorafenib	464.83
5757	Estradiol	272.39	216239	Sorafenib	464.83
5870	Estrone	270.37	5359476	Sulfasalazine	398.39
36462	Etoposide	588.56	5358	Sumatriptan	295.40
151115	Exatecan	435.45	5329102	Sunitinib	398.48
150311	Ezetimibe	409.43	2733526	Tamoxifen	371.52
3385	Fluorouracil	130.08	3038522	Tandutinib	562.71
6037	Folic acid	441.40	148201	Tariquidar	646.74
403923	Fumitremorgin C	379.46	6675	TAUROCHOLIC ACID	515.71
3454	Ganciclovir	255.23	65999	Telmisartan	514.63
123631	Gefitinib	446.98	452548	Teniposide	656.65
5280961	Genistein	270.24	54684141	Teriflunomide	270.21
9577124	Gimatecan	447.49	6013	Testosterone	288.43
5281887	Glucuronosylestradiol	448.51	60700	Topotecan	421.45
124886	Glutathione	307.32	5583	Trimetrexate	369.42
72474	Grepafloxacin	359.40	23696199	Troglitazone Sulfate Sodium	543.58
72281	Hesperetin	302.28	124225	Ulifloxacin	349.38
1066634 6	Homocamptothecin	362.38	1175	Uric acid	168.11
5754	Hydrocortisone	362.47	3081361	Vandetanib	475.36
5291	Imatinib	493.61	42611257	Vemurafenib	489.92
60838	Irinotecan	586.69	5656	Venlafaxine	277.41
5330790	JNJ7706621	394.36	2520	VERAPAMIL	454.61
5280863	Kaempferol	286.24	24776445	Vismodegib	421.29
1032245 0	Ko 143	469.58	4055	Vitamin K3	172.18
60825	Lamivudine	229.25	1188	Xanthine	152.11
3883	Lansoprazole	369.36	5717	Zafirlukast	575.68
208908	Lapatinib	581.06	35370	Zidovudine	267.24
3899	Leflunomide	270.21	3035010	Benzo(a)pyrene-3-O-glucuronide	444.50
9823820	Lenvatinib	426.86	10095558 8	Iodoarylazidoprazosin	545.34

**Table 3. Docking results summary with chemical structures and drug-like activities of selected top ten ATP-binding cassette super family G 2 inhibitors.**

PubChem CID	Chemical structure	Physiochemical Properties	BE	Hydrogen Bonding Interactions		
				No. of Bonds	Interactions	Distance
11937		MW:193.25 HBD:1 HBA:1 RB: 0 TPSA:26	-9.8	1	O1-Thr421:N	2.87
3035010		MW:444.44 HBD:4 HBA:7 RB:3 TPSA:116	-9.5	1	O2-Lys417:NZ	3.04
6037		MW:441.40 HBD:6 HBA:9 RB:9 TPSA:209	-9.6	2	O-Ser563:OG OE1-Lys417:NZ	2.81 3.05
5291		MW:493.61 HBD:2 HBA:7 RB:7 TPSA:86.3	-9.6	2	N4-Thr94:OG1 N4-Thr94:O	3.27 3.12

644241		MW:529.53 HBD:2 HBA:9 RB:6 TPSA:97.6	-9.8	3	N1-Thr94:OG1 O-Lys417:N2 N7-Trp92:NE1	3.10 2.83 3.26
24826799		MW:532.57 HBD:1 HBA:8 RB:6 TPSA:65.8	-9.9	1	O-Ser93:OG	3.11
11167602		MW:482.82 HBD:3 HBA:8 RB:5 TPSA:92.4	-9.9	3	N2-Thr559:N2 O3-Asn604:ND2 N4-Asn604:OD1	3.06 3.14 3.27
216239		MW:464.83 HBD:3 HBA:7 RB:5 TPSA:92.7	-9.9	7	F2-Tyr28:N N2-Val615:O N2-Thr359:OG1 N1-Lys616:O O1-Trp92:NE1 N4-Trp92:O N4-Tyr91:O	3.06 2.92 3.12 3.22 3.18 2.87 3.19
6013		MW:288.43 HBD:1 HBA:2 RB: 0 TPSA:37.3	-9.5	3	O1-Lys616:NZ O1-Thr607:OG1 O1-Tyr605:O	3.16 2.70 2.93

148201		MW:646.74 HBD:2 HBA:8 RB:11 TPSA:111	-9.7	3	O4-Lys417:N2 N3-Thr94:O O3-Lys628:NZ	3.08 2.49 3.16
--------	--	--	------	---	--	----------------------

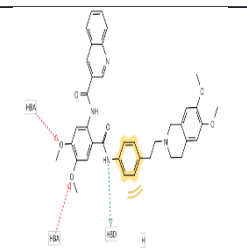
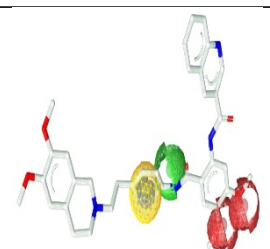
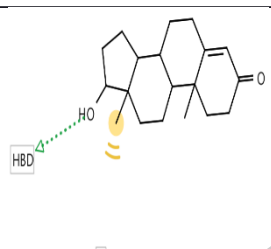
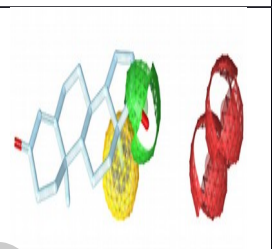
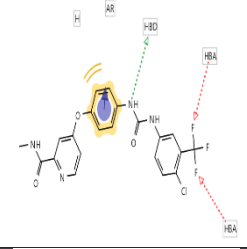
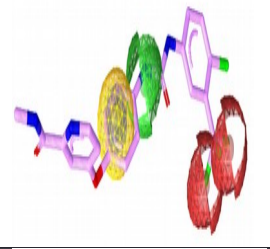
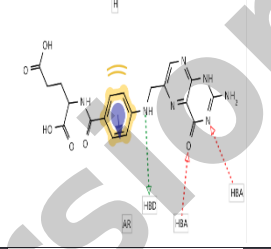
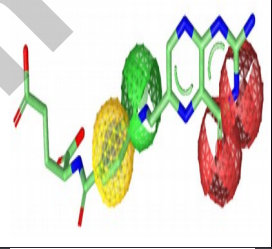
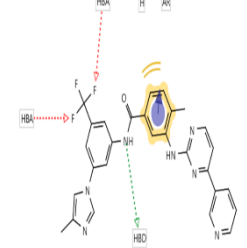
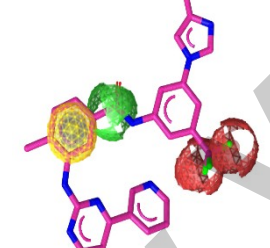
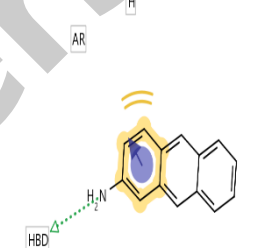
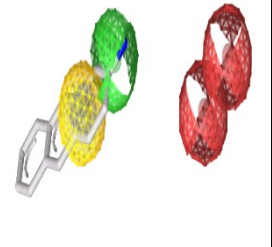
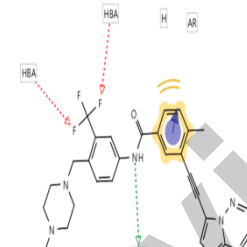
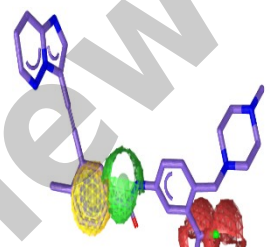
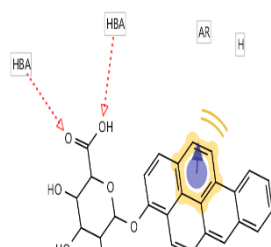
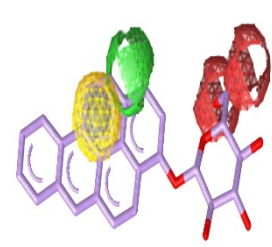
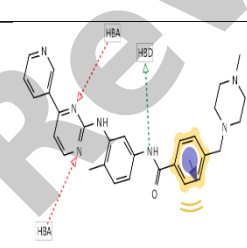
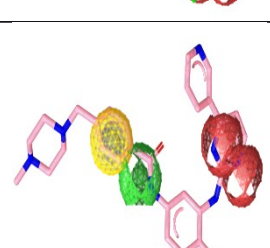
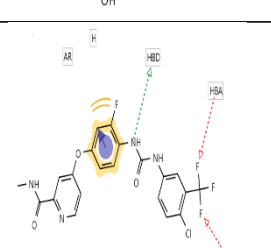

\*(BE: Binding Energies, MW: Molecular Weight (g/mol), HBD: hydrogen bond donor, HBA: hydrogen bond acceptor, RB: rotatable bonds, TPSA: Topological polar surface area)

Review Version

**Table 4. Pharmacophore features of the selected set of ATP-binding cassette super family G 2 inhibitors with their pharmacophore fit scores.**

<b>PubChem CID</b>	<b>HR</b>	<b>AR</b>	<b>HBA</b>	<b>HBD</b>	<b>Number of Confirmations</b>	<b>Common Pharmacophore Feature</b>	<b>Pharmacophore Fit Score</b>
148201	1	6	7	2	25	5	41.86
216239	1	3	6	3	25	5	50.84
644241	1	5	8	2	25	5	50.85
24826799	1	5	6	1	25	5	51.33
5291	1	5	4	2	25	5	51.03
6013	1	4	2	1	1	2	26.02
6037	1	3	9	4	25	5	51.40
11937	1	3	0	1	1	2	34.47
3035010	1	6	7	3	25	4	42.40
11167602	1	3	7	3	25	5	52.14

**Table 5. Overlay of selected set of ATP-binding cassette super family G 2 inhibitors upon the Pharmacophore model generated by LigandScout 4.1.5.**

PubChem CID	2D Pharmacophore	3D Pharmacophore	PubChem CID	2D Pharmacophore	3D Pharmacophore
148201			6013		
216239			6037		
644241			11937		
2482679 9			3035010		
5291			1116760 2		



**Table 6. Docking results of top 10 scored virtual hits screened from Zbc library of ZINC database.**

ZINC ID's	Binding energies	Hydrogen bonding interactions		
		No. of bonds	Interactions	Distance
44740	-8.5	2	O1-Asn604:ND2 N1-Try91: O	2.80 3.31
2125703	-7.3	2	N1-Thr607:OG1 O4-Thr607:OG1	3.34 3.10
4037390	-8.1	2	N1-Asp419:OD1 N1-Try51:OH	3.07 3.05
4098704	-8.5	4	O6-Gln424:N O2-Thr607:OG1 O3-Thr607:OG1 O4-Lys616:NZ	2.93 3.20 2.95 2.79
4260210	-7.6	2	N1-Ser420: O O1-Thr607:OG1	3.00 2.75
4270937	-8.3	6	O1-Lys616:NZ O1-Thr607:OG1 O3-Gln424:N N4-Ser420: O O4-Thr607:OG1 O4-Lys616:NZ	3.11 2.78 2.98 3.17 2.73 3.10
15674632	-8.4	2	O2-Lys616:NZ O2-Tyr605: O	3.08 3.05
20412614	-8	2	O3-Lys616:NZ O5-Gln424:N	3.06 3.21
31159138	-8.4	4	O2-Asp419:OD2 O2-Thr94:OG1 O3-Thr94:N O3-Trp92: O	2.72 3.09 3.26 2.94
68606591	7.8	No	No	No

**Table 7. Pharmacological properties of top 10 scored virtual hits screened from Zbc library of ZINC database.**

ZINC ID's / Properties	44740	2125703	4037390	4098704	4260210	4270937	15674632	20412614	31159138	68606591
<b>BBB</b>	0.8978	0.8672	0.8541	0.7589	0.8382	0.8775	0.5493	0.6000	0.5933	0.7436
<b>HIA</b>	0.5139	0.6296	0.9584	0.7279	1.0000	0.9766	0.9723	0.6179	0.9843	0.9348
<b>Caco-2</b>	0.9287	0.9533	0.7685	0.5328	0.9029	0.5722	0.366	0.5182	0.3121	0.5274
<b>CYP450 2D6 substrate</b>	0.8111	0.7289	0.8389	0.9134	0.7376	0.8098	0.7632	0.7271	0.8671	0.8448
<b>AMES-Tox</b>	0.6258	0.6294	0.5592	0.6259	0.5868	0.5969	0.5566	0.7421	0.6523	0.8631
<b>Carcinogenic</b>	0.9287	0.9017	0.8137	0.9037	0.9395	0.9235	0.9235	0.9411	0.9467	0.6314
<b>MW</b>	341.36	332.3	304.26	283.21	294.35	318.33	337.4	332.33	344.36	315.26
<b>LogP</b>	-0.87	-0.85	1.9	-1.53	-0.38	-0.13	0.24	-0.77	0.51	-0.31
<b>HBD</b>	2	1	2	2	1	2	2	2	4	1
<b>HBA</b>	4	5	4	6	3	4	5	5	6	6
<b>RB</b>	8	9	2	3	3	3	6	9	5	6
<b>Rings</b>	3	2	4	3	3	3	4	2	4	2
<b>PSA</b>	107.18	108.67	117.32	114.73	72.96	90.98	75.28	119.67	115.06	130.27

\*(BBB: Blood Brain Barrier, HIA: Human Intestinal Absorption, Caco2: Caco-2 Permeability, MW: Molecular Weight, HBD: Hydrogen Bond Donors, HBA: H-Bond Acceptors, RB: Rotatable Bonds, PSA: Polar Surface Area)

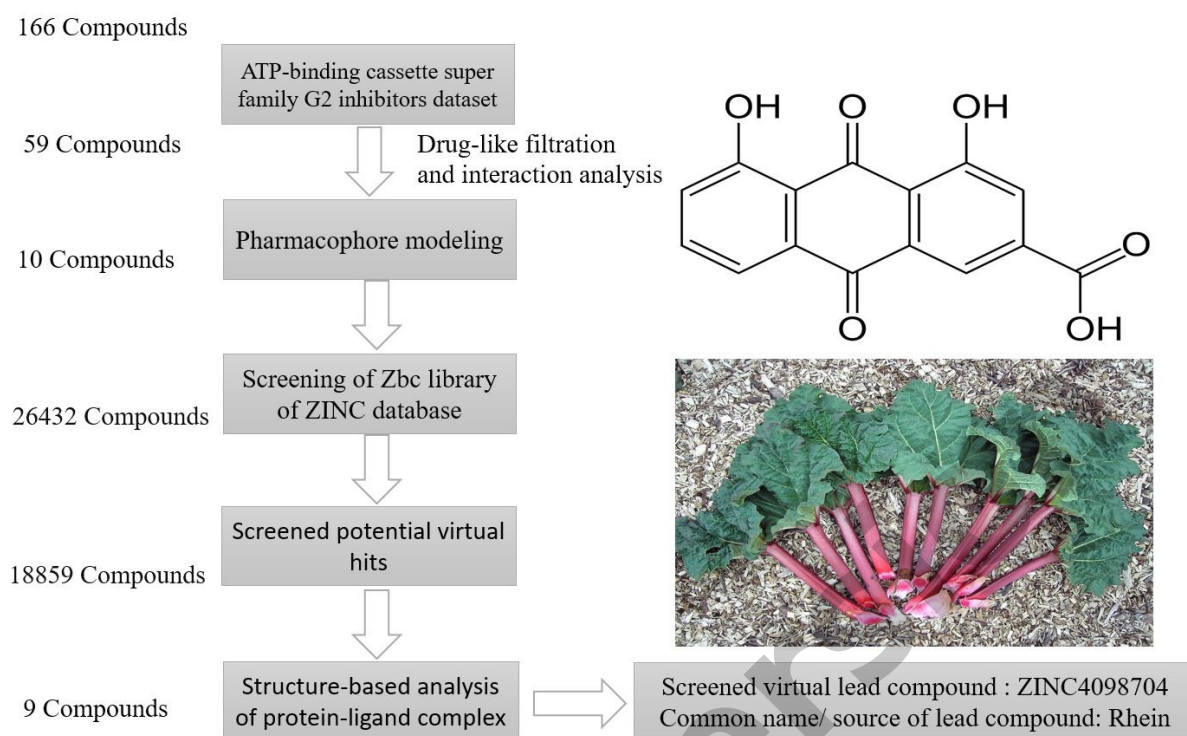


**Figure 1.** Computer-aided drug design scheme used to screen ATP-binding cassette super family G 2 inhibitors to control multidrug resistance in treatment of cancer

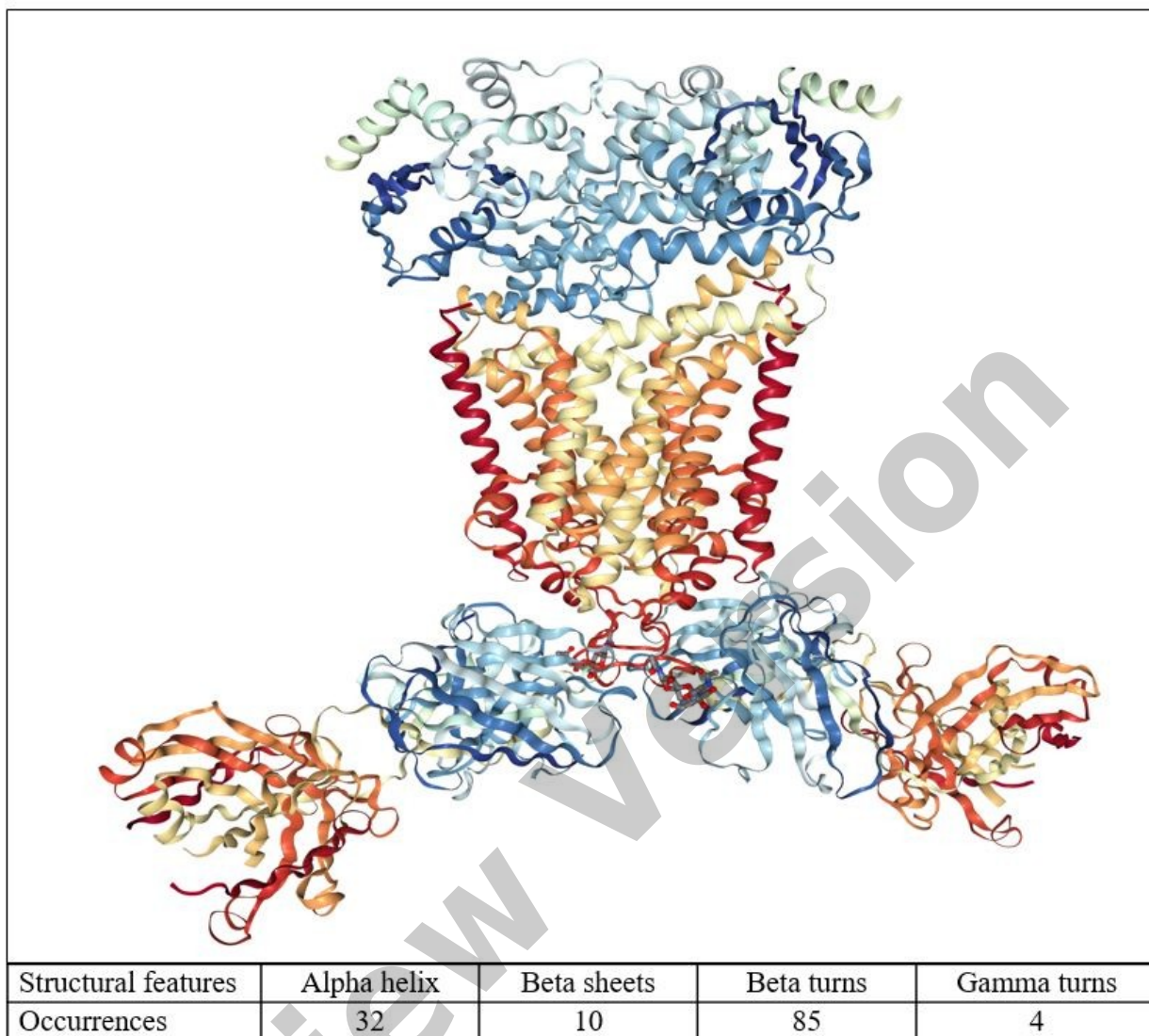
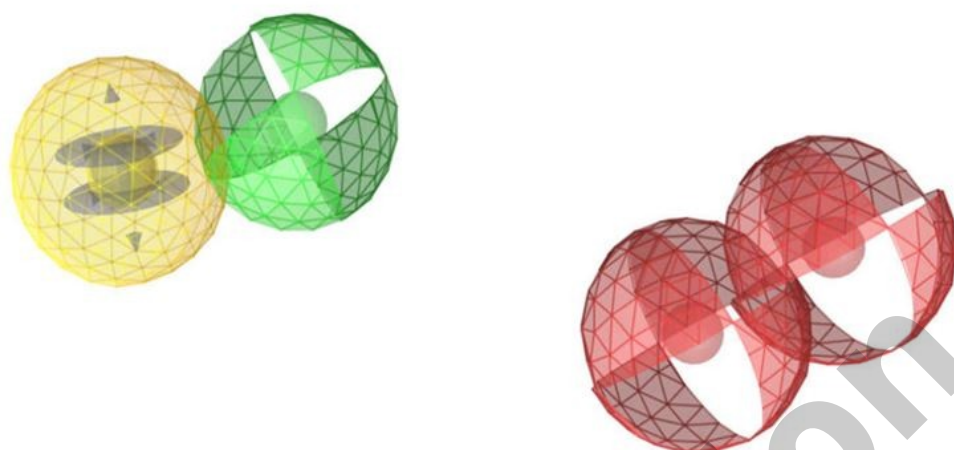


**Figure 2.** Three-dimensional structure of ATP-binding cassette super family G 2 protein with its structural features generated by chimera tool



Name	Score	Name	Score	Name	Score	Name	Score	Name	Score
Model-1	0.6872	Model-3	0.6785	Model-5	0.6605	Model-7	0.6540	Model-9	0.6373
Model-2	0.6862	Model-4	0.6784	Model-6	0.6550	Model-8	0.6394	Model-10	0.6083

**Figure 3.** Lower panel shows ten pharmacophore models scores of selected ATP-binding cassette super family G2 inhibitors generated by LigandScout 4.1.5. Upper panel shows the proposed pharmacophore model shows five common features to generate the best pharmacophore model contains two red spheres (hydrogen bond acceptors), one green sphere (hydrogen bond donor), a yellow sphere having a blue small sphere (hydrophobic region with an aromatic ring).

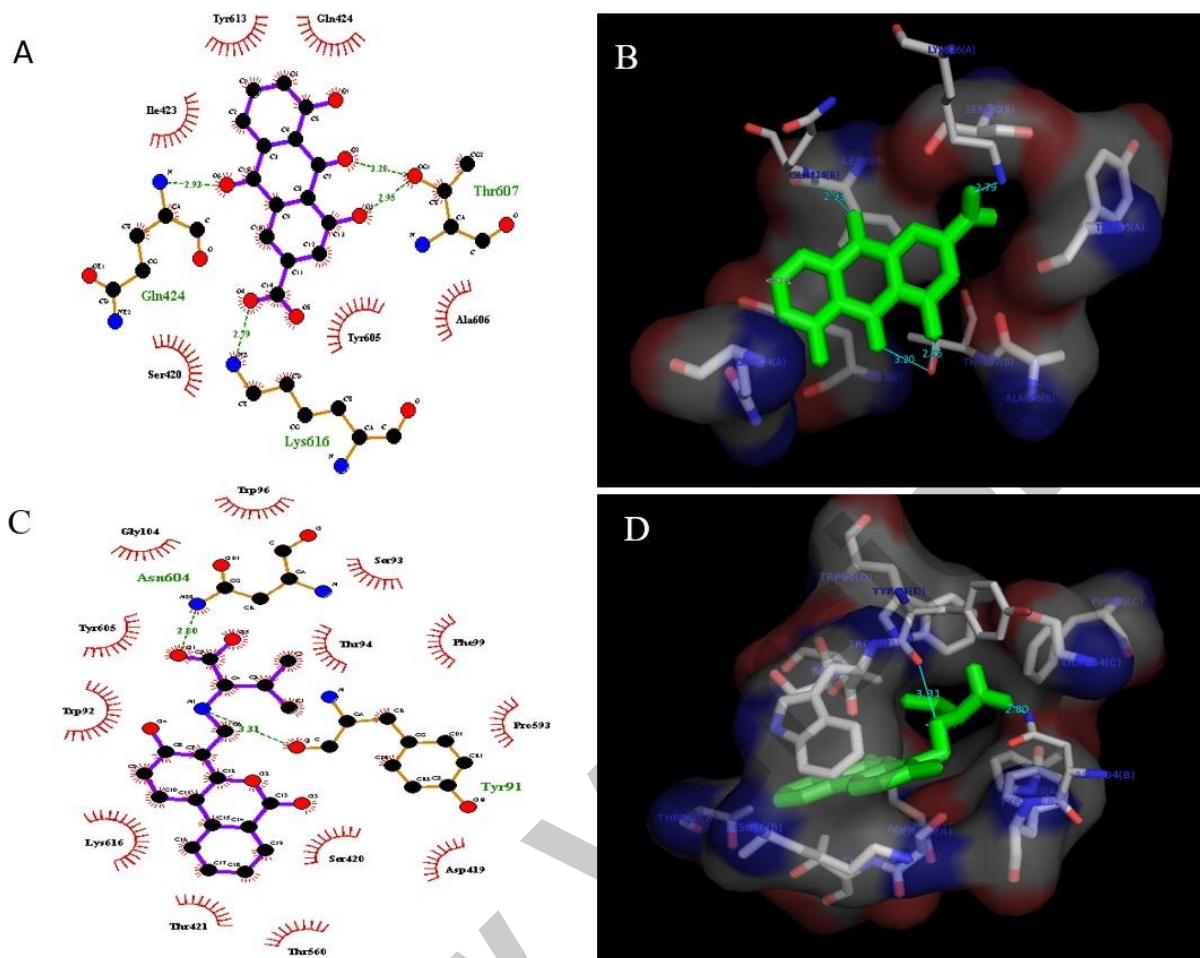


**Figure 4.** Binding interactions of ZINC4098704 [A, B] and ZINC44740 [C, D] with ATP-binding cassette super family G 2 protein [PDB ID: 5NJ3], [A] and [C] demonstrates two dimensional plots while [B] and [D] demonstrates the ligands interactions in three dimensional binding cavity of target protein [23].

REVIEW